Article

Bilayers and Interdigitation in Block Copolymer Vesicles

Giuseppe Battaglia, and Anthony J. Ryan

J. Am. Chem. Soc., **2005**, 127 (24), 8757-8764• DOI: 10.1021/ja050742y • Publication Date (Web): 27 May 2005

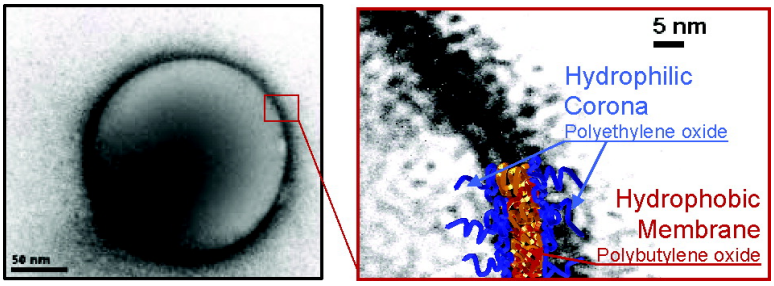

More About This Article

Additional resources and features associated with this article are available within the HTML version:

- Supporting Information
- Links to the 18 articles that cite this article, as of the time of this article download
- Access to high resolution figures
- Links to articles and content related to this article
- Copyright permission to reproduce figures and/or text from this article

View the Full Text HTML

J|A|C|S
ARTICLES
Published on Web 05/27/2005

Bilayers and Interdigitation in Block Copolymer Vesicles

Giuseppe Battaglia and Anthony J. Ryan*

Contribution from the Department of Chemistry, University of Sheffield, Sheffield, U.K. S3 7HF

Received February 4, 2005; E-mail: a.ryan@shef.ac.uk

Abstract: Amphiphilic block copolyethers assemble into membranes with thickness between 2.4 and 7.5 nm. The vesicular morphology has been confirmed by small-angle X-ray scattering combined with electron microscopy for diblock copolymers and triblock copolymers of both architectures. The scaling of the membrane thicknesses with the length of the hydrophobic block is in good agreement with the strong segregation theory for block copolymer melts, indicating a mixed and stretched conformation of the hydrophobic chain inside the vesicle membrane. This result is in contrast to previously published results where the hydrophobic membranes were observed to have bilayer geometry and polymer chains that are relatively unperturbed from their ideal Gaussian dimensions.

Introduction

The ability of natural phospholipids to assemble into membranes and specifically into vesicles has recently been mimicked by synthetic amphiphilic block copolymers in both water[1,2] and organic solvents.[3] The wholly synthetic nature of these copolymer vesicles, known as polymersomes,[4] allows a wide range of chemistry to be applied in the design of mechanically and chemically enhanced membranes with a flexible range of diameters and membrane thicknesses.

Phospholipids are known to exhibit a large number of phases in water whose morphologies change not only in terms of long-order organization but also in terms of short-range organization.[5] Normally phospholipids assemble into membranes with a very ordered bilayer structure, typical of solid phases, having a thickness[6] between 4 and 5 nm. Such a structure, known as β conformation, arises from the intersection of two phospholipid monolayers that contact each other at the hydrophobic chain-end while their hydrophilic headgroups interact with the water. Hydrocarbon chains assume different conformations as a function of different parameters such as temperature,[7] osmotic pressure,[8] or hydrotrope addition.[9,10] The membrane transforms from an ordered bilayer into a more disordered and interdigitated structure, typical of liquid phases, known as α conformation (Figure 1a), where the terminal group of the hydrophobic chain protrudes beyond the bilayer midline to interpenetrate the opposite bilayer, and as consequence, the membrane thickness is almost halved.

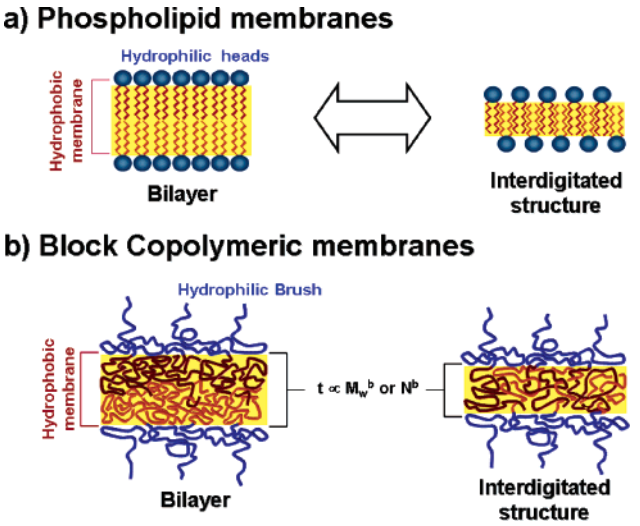

Figure 1. (a) Phospholipids can assemble into bilayer membranes and under particular conditions into interdigitated membranes. (b) By analogy, block copolymers can assemble in similar structures. The hydrophobic membrane is shielded from water by a polymeric brush made of the partial coiling[15] of the hydrophile. The higher molecular weight hydrophobic polymer coils are more likely to interdigitate and become entangled.

In Figure 1 both the phospholipid and the polymeric membranes have been represented with the two monolayers having different colors. The bilayer geometry is a highly ordered structure that necessitates a low-entropy conformation; it can be taken up by short chain molecules, such as the phospholipids. The analogy between polymeric membranes and lipid bilayer membranes is rather easy to make, and the literature reinforces this connection repeatedly.[1,4,11] The similarities observed, however, may be quantitatively inappropriate at higher molec-

(1) Discher, D. E.; Eisenberg, A. *Science* **2002**, *297*, 967−973.
(2) Kabanov, A. V.; Bronich, T. K.; Kabanov, V. A.; Yu, K.; Eisenberg, A. *J. Am. Chem. Soc.* **1998**, *120*, 9941−9942.
(3) Ilhan, F.; Galow, T. H.; Gray, M.; Clavier, G.; Rotello, V. M. *J. Am. Chem. Soc.* **2000**, *122*, 5895−5896.
(4) Discher, B. M.; Won, Y.-Y.; Ege, D. S.; Lee, J. C.-M.; Bates, F. S.; Discher, D. E.; Hammer, D. A. *Science* **1999**, *284*, 1143−1146.
(5) Luzzati, V.; Tardieu, A. *Annu. Rev. Phys. Chem.* **1974**, *25*, 79−94.
(6) Cevc, G.; Marsh, D. *Phopsholipid Bilayers: Physical Principles and Models*; John Wiley & Sons: New York, 1987; Vol. 5.
(7) Seddon, J. M.; Cevc, G.; Kaye, R. D.; Marsh, D. *Biochemistry* **1984**, *23*, 2634−2644.
(8) Yamazaki, M.; Ohshika, M.; Kashiwagi, N.; Asano, T. *Biophys. Chem.* **1992**, *43*, 29−37.
(9) Breen, R. L. M. a. J. J. *Langmuir* **2001**, *17*, 5121−5124.
(10) Boon, J. M.; McClain, R. L.; Breenb, J. J.; Smitha, B. D. *J. Supramol. Chem.* **2001**, *1*, 17−21.
(11) Luo, L.; Eisenberg, A. *J. Am. Chem. Soc.* **2001**, 1012−1013.

ular weights. In fact the nomenclature of bilayers and interdigitation brings with it some prejudice from the phospholipid arena. The behavior of block copolymer lamellae in the melt shows us that the two stretched brushes,[12−14] emanating from the interfaces and comprising each domain, are mixed for entropic reasons. Rather than asking, is the membrane a bilayer or is it interdigitated, an alternative question might be, what could drive autophobic demixing (Figure 1b) of two identical polymer brushes? Because this is what a bilayer means in terms of polymer physics.

For polymeric membranes the configurational entropy penalty for demixing the two layers is high compared to mixing and stretching, and this was clearly shown in a self-consistent-field calculation[16] testing the strong segregation theory. This calculation clearly shows that the majority of end segments pass the midplane at segregation strengths similar to those observed herein. In fact strongly stretched brushes (and a clear bilayer with no interdigitation) are only anticipated in the limit of infinite segregation strength, i.e., $\chi N = \infty$, where χ is the Flory−Huggins interaction parameter and N is the degree of polymerization. The formation of lamellar structures and amphiphilic membranes can be explained using the critical packing factor and the curvature models,[11,17] which are based on geometrical considerations. Thermodynamically, the self-assembly of amphiphilic molecules can be explained using to two main contributions to the free energy: the interfacial tension of the hydrophobic/hydrophilic boundary and the entropic loss when the polymeric chains are forced into more ordered structures. When there is a mismatch between the interfacial tension and the entropic stretching penalty, the minimization of the interfacial surface governs the association thermodynamics. At this point, known as the strong segregation limit,[18] the hydrophobic and the hydrophilic phases are well separated and the chains strongly stretched. In lamellar structures or membranes, the strength of segregation can be measured, on the basis of how the lamellar spacing, d, or the membrane thickness, t, varies with the number of hydrophobic units, N. Assuming a power law between t and N, such as $t \sim N^b$, the exponent b can used to infer the segregation strength. One of the boundary conditions, fully stretched chains, would give $b = 1$, and this is the theoretical limit approached by phospholipids. The other boundary condition, a random (Gaussian) coil, would give $b = 1/2$, and this is known as weak segregation in block copolymer melts. In the intermediate condition known as strong segregation, the exponent[19] is $b = 2/3$. The prediction for the scaling of the spacing with molecular weight has been demonstrated many times experimentally[13,20−22] for block copolymers in bulk. Amphiphilic block copolymers assembled into spherical and wormlike micelles in selective solvents have also been shown[23−25] to have aggregate radii that vary in agreement with the strong segregation regime. In fact the scaling behavior found for micelles suggests that they are in the superstretched[26] limit with $b \approx 4/5$. In particular, Discher[27] et al. have studied the assembly of poly(ethylene oxide)-*co*-1,2 polybutadiene into wormlike micelles reporting a scaling of the radius with the number of hydrophobic units in good agreement with the strong segregation regime (exponent $b = 0.61$). The same group, however, performed a similar study[28] on polymeric vesicles using the same block copolymer system, and in contrast the membrane thickness, t, presented a scaling with N with an exponent $b = 1/2$. This result suggests that the hydrophobic chains are relatively unperturbed from their ideal state. In an cryogenic electron microscopy study[29] that focused on the nonergodic nature of block copolymer assembly, Bates and co-workers suggested, for a smaller range of molecular weights, that a 2/3 power law applies to hydrophobe dimensions for aggregates that are spherical, wormlike, and vesicular.

Table 1. Copolymer Characteristics: f_E Is the Volume Fraction of the E Block; M_w Is the Block Copolymer Molecular Weight Calculated[12] by GPC and ^{13}C NMR

copolymer		f_E	M_w
E_NB_M diblock	$E_{16}B_{22}$	0.270	2300
	$E_{50}B_{70}$	0.280	7300
	$E_{68}B_{65}$	0.361	7700
	$E_{115}B_{103}$	0.371	12500
$B_ME_NB_M$ triblock	$B_{37}E_{77}B_{37}$	0.355	8700
	$B_{46}E_{99}B_{46}$	0.363	11000
$E_NB_ME_N$ Triblock	$E_{31}B_{54}E_{31}$	0.378	6600
	$E_{34}B_{75}E_{34}$	0.324	8400
	$E_{40}B_{100}E_{40}$	0.336	11400
	$E_{32}B_{114}E_{32}$	0.245	11300

In the present work, E_M denotes an oxyethylene block [E = OCH_2CH_2] prepared from ethylene oxide, and B_N an oxybutylene block [B = $OCH_2CH(C_2H_5)$] prepared from 1,2-butylene oxide, where M and N denote number-average block lengths. Thus a diblock copolymer is denoted E_MB_N, and a triblock copolymer either $E_MB_NE_M$ or $B_NE_MB_N$. These polymers, previously characterized in water[12] and in bulk,[13] have been selected to study self-assembly into polymeric vesicles, specifically the relationship between the molecular size and the membrane thickness. The molecular details of the copolymers are listed in Table 1.

Result and Discussions

To assess the block copolymers ability to form vesicles, both giant vesicles (microscale) and nano-vesicles have been generated using different techniques originally developed for phospholipids.[30,31] All the amphiphilic copolyethers listed in Table

(12) Hamley, I. W.; Mai, S.-M.; Ryan, A. J.; Fairclough, J. P. A.; Booth, C. *Phys. Chem. Chem. Phys.* **2001**, *3*, 2972−2980.
(13) Ryan, A. J.; Mai, S.-M.; Fairclough, J. P. A.; Hamley, I. W.; Booth, C. *Phys. Chem. Chem. Phys.* **2001**, *3*, 2961−2971.
(14) Shull, K. R.; Mayes, A. M.; Russell, T. P. *Macromolecules* **1993**, *26*, 3929−3936.
(15) Zheng, Y.; Won, Y.-Y.; Bates, F. S.; Davis, H. T.; Scriven, L. E.; Talmon, Y. *J. Phys. Chem. B* **1999**, *103*, 10331−10334.
(16) Matsen, M. W.; Bates, F. S. *Macromolecules* **1995**, *28*, 8884−8886.
(17) Israelachivili, J. N. *Intermolecular & Surface Forces*, 9th ed.; Elsevier Science Imprint: London, 2002.
(18) Bates, F. S.; Fredrickson, G. H. *Annu. Rev. Phys. Chem.* **1990**, *41*, 525−557.
(19) Matsen, M. W.; Bates, F. S. *Macromolecules* **1996**, *29*, 1091−1098.
(20) Hadziioannout, G.; Skoulios, A. *Macromolecules* **1982**, *15*, 258−262.
(21) Hashimoto, T.; Shibayama, M.; Kawai, H. *Macromolecules* **1980**, *13*, 7−1247.
(22) Richards, R. W.; Thomasont, J. L. *Macromolecules* **1983**, 982−992.
(23) Forster, S.; Zisenis, M.; Wenz, E.; Antonietti, M. *J. Chem. Phys.* **1996**, *104*, 9956−9970.
(24) Nagarajan, R.; Ganesh, K. *J. Chem. Phys.* **1989**, *90*, 5843−5856.
(25) Noolandi, J.; Hong, K. M. *Macromolecules* **1983**, *16*, 1443−1448.
(26) Semenov, A. N.; Nyrkova, I. A.; Khokhlov, A. R. *Macromolecules* **1995**, *28*, 7491−7500.
(27) Dalhaimer, P.; Bermudez, H.; Discher, D. E. *J. Polym. Sci.: Part B: Polym. Phys.* **2004**, *42*, 168−176.
(28) Bermudez, H.; Brannan, A. K.; Hammer, D. A.; Bates, F. S.; Discher, D. E. *Macromolecules* **2002**, *35*, 8203−8208.
(29) Jain, S.; Bates, F. S. *Macromolecules* **2004**, 1511−1523.
(30) Luisi, P. L.; Walde, P. *Giant Vesicles*; John Wiley & Sons Ltd: Chichester, 2000.
(31) Lee, J. C.-M.; Bermudez, H.; Discher, B. M.; Sheehan, M. A.; Won, Y.-Y.; Bates, F. S.; Discher, D. E. *Biotechnol. Bioeng.* **2001**, *73*, 135−145.

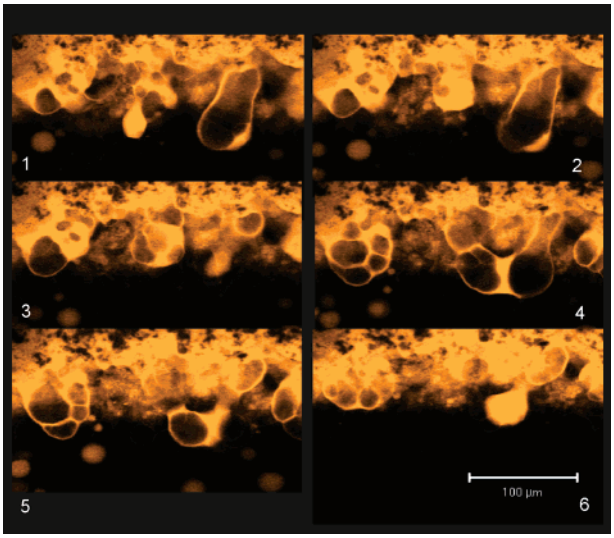

Figure 2. $E_{16}B_{22}$ unilamellar vesicle formation monitored by confocal laser scanning microscope. Amphiphilic dye, Rhodamine B octadecyl ester perchlorate, has been added to highlight the membranes.

1 have shown high propensity to form vesicles. Particularly, they have been able to generate giant vesicles, whose size allows investigation of their formation and the behavior of single supramolecular entities using light microscopy.

In Figure 2, six confocal laser scanning micrographs, taken at different times, show the electroformation[32] and the detachment of $E_{16}B_{22}$ vesicles from platinum electrode surfaces. Application of the ac field causes membranes to start budding from the surface of the copolymer film. These membranes undergo deformation and fuse together. Eventually, they enclose into vesicles and detach from the electrode. Vesicles form readily from EB copolymers; however, the time when the first vesicle is observed depends strongly on the polymer molecular weight. Low molecular weight block copolymers take a few minutes, whereas those of high molecular weight can take up to a few hours, indicating a strong dependence of the membrane flexibility on the molecular weight.

At a different scale, nano-vesicles have been generated using rehydration techniques, and their size distribution has been controlled by further sonication or extrusion. The energetic penalty for spherical vesicle formation is independent of the radius, being the sum of the mean and Gaussian curvature, so energy input through sonication or extrusion results in the formation of smaller stable vesicles. All EB copolymer vesicles have shown very long shelf life, and no visual phase separation has been observed. Dynamic light scattering (DLS) has not revealed dramatic differences in the particle size distribution even after months, as represented in Figure 3. DLS measurements have also revealed that most of the aggregates have size greater than 30 nm. This is strong evidence of the absence of spherical micelles, which are generally much smaller.

Vesicle geometry and its membrane morphology have been assessed by transmission electron microscopy (TEM) and small-angle X-ray scattering (SAXS). The former gives real space images with rather high resolution, but it has the intrinsic disadvantage that the sample preparation may introduce artifacts. To minimize the effect of artifacts, three techniques have been

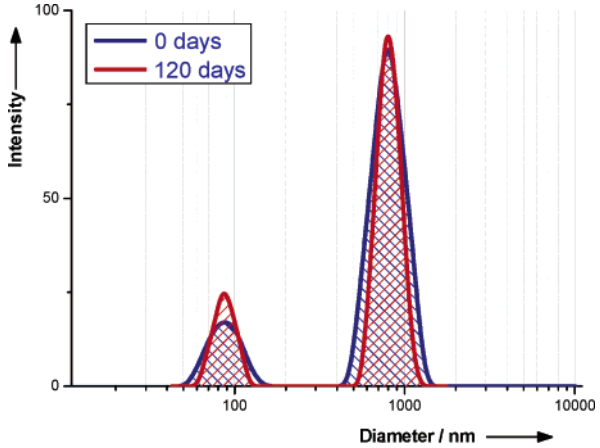

Figure 3. $E_{16}B_{22}$ vesicle dispersion DLS particle size distribution measured right after preparation and after 120 days from preparation.

employed to prepare TEM samples: freeze-drying, negative staining, and cryogenic electron microscopy. Freeze-drying techniques allow very rapid preparation and observation of the copolymer vesicle dispersions. The sample is first frozen and then placed under high vacuum overnight. Nevertheless, the water is mainly removed by sublimation and therefore very rapidly; this technique cannot be applied for very sensitive and unstable vesicles, such as most phospholipid vesicles. In Figure 4, two different micrographs taken from freeze-dried samples at different magnification show that the main aggregate has the vesicular geometry, only very few nonvesicular aggregates being observed. EB vesicles have also proven to keep their spherical shape, and at high magnification the core-shell morphology can be observed clearly. This indicates high stability of the aggregate even under drastic water removal conditions.

Complementarily to freeze-drying, the vesicle dispersions have been negatively stained with uranyl acetate. Such heavy metal ions are used as they fix organic structures at the molecular level extremely rapidly[33] (~10 ms), arresting structural changes in macromolecules due to drying effects, and they interact with the electron beam, producing phase contrast. In the negative stained micrographs of $E_{50}B_{70}$ and $E_{16}B_{22}$ vesicles in Figure 5, the presence of uranyl acetate highlights the hydrophobic membrane and, with less resolution, the hydrophilic corona. As shown in the magnification boxes in Figure 5, the hydrophobic membrane boundary can be easily identified, and therefore its thickness can be measured very accurately, provided a correct calibration of the electron microscope.

Freeze-drying and negative staining both require water removal from the sample, and although EB copolymeric vesicles have proven high stability, the most ideal technique for observing the vesicle in its own environment is cryogenic transmission electron microscopy. The sample is first vitrified by rapid immersion in liquid ethane and then kept at about −170 °C throughout TEM observation. The micrographs in Figure 6 show the vitrified $B_{37}E_{77}B_{37}$ and $E_{40}B_{100}E_{40}$ vesicle dispersions; the vesicle thicknesses were calculated using the method described in ref 28, and this is demonstrated as an inset to the figure. As well as other TEM techniques and DLS, very little evidence of nonvesicular aggregates has been observed.

Scattering experiments[34] give reciprocal space structure over a large volume and the structural information is averaged over

(32) Menger, F. M.; Angelova, M. I. *Acc. Chem. Res.* **1998**, 789−797.

(33) Zhao, F.-Q.; Craig, R. *J. Struct. Biol.* **2003**, *141*, 43−52.

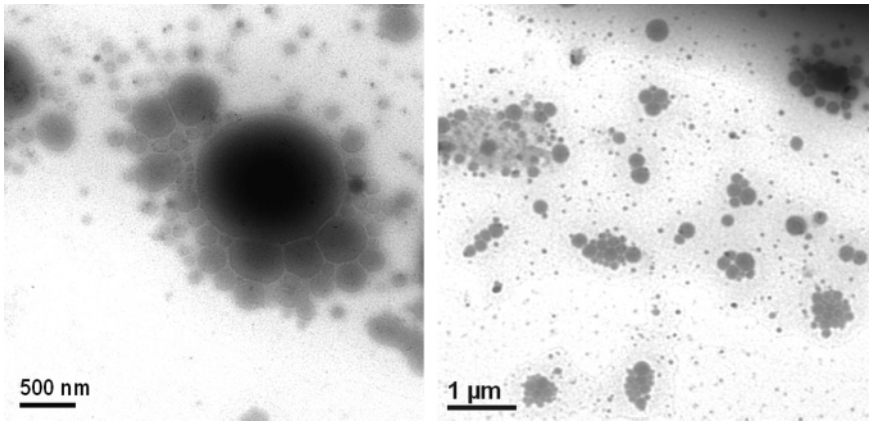

Figure 4. Transmission electron micrograph of freeze-dried $E_{16}B_{22}$ vesicle dispersion. Both pictures show, at two different magnifications, that the majority of aggregates are vesicles.

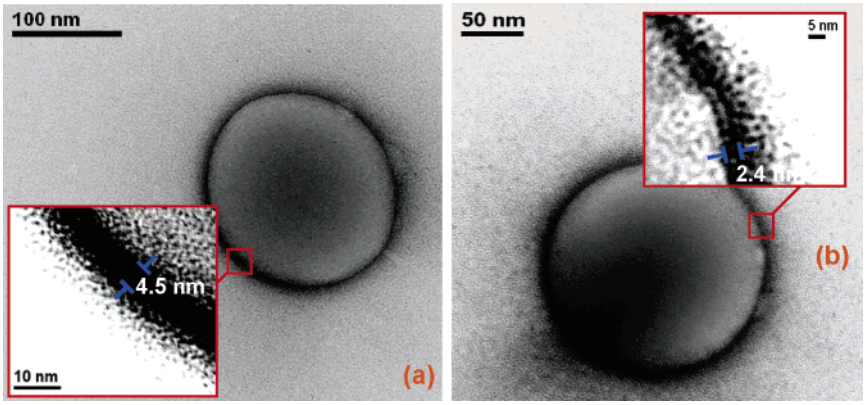

Figure 5. Transmission electron micrograph of negative stained $E_{50}B_{70}$ (a) and $E_{16}B_{22}$ (b) vesicle dispersions. Both pictures show, at two different magnifications, the morphology of the hydrophobic membrane and the hydrophilic corona.

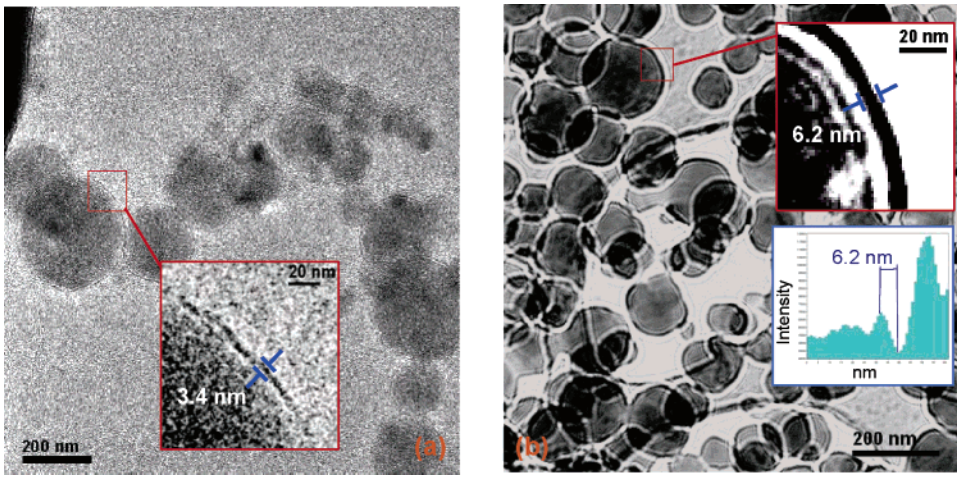

Figure 6. Cryogenic transmission electron micrograph of $B_{37}E_{77}B_{37}$ (a) and $E_{40}B_{100}E_{40}$ (b) vesicle dispersions. Both pictures show, at two different magnifications, the membranes. In part b, the experimental intensity profile of the vesicle membrane is plotted and, using the method in ref 28, the thickness can be calculated.

a large number of macromolecular aggregates in solution. Such information is strongly dependent on both the polydispersity of the aggregates and on the homogeneity of the solution. As a consequence, SAXS experiments can show which type of aggregate (vesicles, wormlike, and spherical micelles) the majority of the material is involved in.

The TEM in Figures 5 and 6 show clearly that the vesicles have a uniform membrane thickness but a distribution in diameter. The points in the SAXS pattern in Figure 7a are the experimental data, and the dotted line in Figure 7a is the scattering envelope calculated for a monodisperse vesicle with the average thickness obtained from the scattering and TEM. It shows how the measured data compares well with the calculated scattering from a monodisperse vesicle with the appropriate

(34) Linder, P.; Zemb, T. *Neutrons, X-rays and Light: Scattering Methods Applied to Soft Matter*; Elsevier Science B.V.: Amsterdam, 2002.

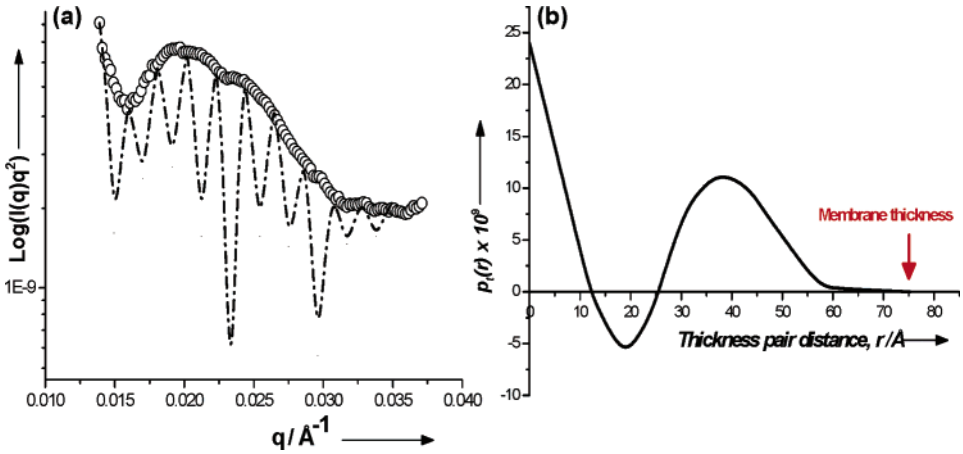

Figure 7. (a) One-dimensional SAXS pattern from (○) $E_{115}B_{103}$ vesicle dispersion and (−•−) the π/r modulation of a monodisperse vesicle dispersion with $r = 298$ nm and a membrane thickness of 7.5 nm. (b) Thickness pair distance function of $E_{115}B_{103}$ vesicle dispersion calculated by the IFT method. The arrow indicates the membrane thickness.

Table 2. EB Vesicle Membrane Thicknesses Calculated Using SAXS Analysis and TEM Analysis

	hydrophobic membrane thickness/nm			
copolymer	SAXS	TEM negative staining (10 vesicles)	TEM cryogenic (10 vesicles)	average
$E_{16}B_{22}$	2.30 ± 0.43	2.51 ± 0.18	2.42 ± 0.16	2.40 ± 0.26
$E_{50}B_{70}$	4.40 ± 0.76	4.36 ± 0.17	4.84 ± 0.39	4.53 ± 0.44
$E_{68}B_{65}$	4.10 ± 0.78	4.05 ± 0.26	4.06 ± 0.19	4.07 ± 0.41
$E_{115}B_{103}$	7.50 ± 1.03	7.53 ± 0.28	7.65 ± 0.39	7.56 ± 0.56
$B_{37}E_{77}B_{37}$	3.20 ± 0.56	3.14 ± 0.16	3.10 ± 0.16	3.15 ± 0.29
$B_{46}E_{99}B_{46}$	3.60 ± 0.62	3.56 ± 0.20	3.10 ± 0.16	3.42 ± 0.33
$E_{31}B_{54}E_{31}$	4.10 ± 0.67	4.17 ± 0.12	4.20 ± 0.18	4.16 ± 0.32
$E_{34}B_{75}E_{34}$	4.60 ± 0.78	4.59 ± 0.22	4.67 ± 0.22	4.62 ± 0.41
$E_{40}B_{100}E_{40}$	6.30 ± 0.98	6.34 ± 0.12	6.46 ± 0.19	6.37 ± 0.43
$E_{32}B_{114}E_{32}$	7.40 ± 1.02	7.38 ± 0.13	7.47 ± 0.23	7.42 ± 0.46

thickness. The scattering of a sphere is a Bessel function with maxima and minima (0) at characteristic values of qR, were q is the scattering vector and R the particle radius. For different values of R these maxima and minima appear at different q values, so if there is a distribution in R, then the scattering pattern is a smooth function as the maxima and minima average out. For spheres, a polydispersity in radius of 10% is sufficient to completely smooth the scattering pattern observed. The scattering from a vesicle is a more complex Bessel function that depends on both the vesicle radius and the membrane thickness.[35] If the diameter of the vesicle was varied (at a constant membrane thickness), the calculated maxima and minima appear at different positions, and if the distribution of diameters was appropriately sampled, the average scattering could assume the shape of the measured pattern. However, extracting both the membrane thickness and the vesicle diameter from such a scattering pattern is an ill-posed problem that does not have a unique solution. That there is a unique membrane thickness is obvious from the TEM, and this thickness is readily corroborated by the scattering from a large ensemble of vesicles.

SAXS patterns are the result of two contributions: the structure factor or interference function, which depends on the interaction between the particles; and the pair distance distribution function (PDDF), which depends on the geometry and shape of the particle. The latter function can be calculated by means of inverse Fourier transformation methods.[36] In X-ray scattering the structural information is the result of contrast in electron density. The aqueous PEO does not have a particularly high contrast with water; therefore, the majority of the contrast comes from the hydrophobic membrane with water. Since EB copolymeric vesicles have a radius of curvature much larger than the membrane thickness, PDDF gives the value of the hydrophobic membrane thickness. The pair distance distribution function obtained from the graph 7a data is given in Figure 7b; the third intercept with the x-axis is the magnitude of the hydrophobic membrane thickness.

In Table 2 the membrane thickness values calculated using the techniques described above are listed. SAXS data and TEM data are in good agreement with each other, although the latter technique seems to have smaller error. However, the TEM errors have been calculated by standard deviation, while SAXS errors are σ^2 from the indirect Fourier transform. In particular, the two values from $E_{31}B_{54}E_{31}$ and $E_{34}B_{75}E_{34}$ are very similar to the value reported by Shillen[37] from another copolyether, the PEO_5-PPO_{68}-PEO_5 vesicles. However, the PPO is less hydrophobic than PBO, and the hydrophilic polymer volume fraction chosen was around 10%, which is more suitable for inversed structures. As a consequence, the stability of such vesicles was reported to be very low in contrast to the present work.

The bulk phase behavior of the EB polymers in both molten and solid state has been studied previously.[13] EB block

(35) Laggner, P. In *Small-Angle X-ray Scattering*; Glatter, O., Kratky, O., Eds.; Academic Press: London, 1982.

(36) Glatter, O.; Kratky, O. *Small-Angle X-ray Scattering*; Academic Press: London, 1982.

(37) Schillén, K.; Bryskhe, K.; Mel'nikova, Y. S. *Macromolecules* **1999**, *32*, 6885−6888.

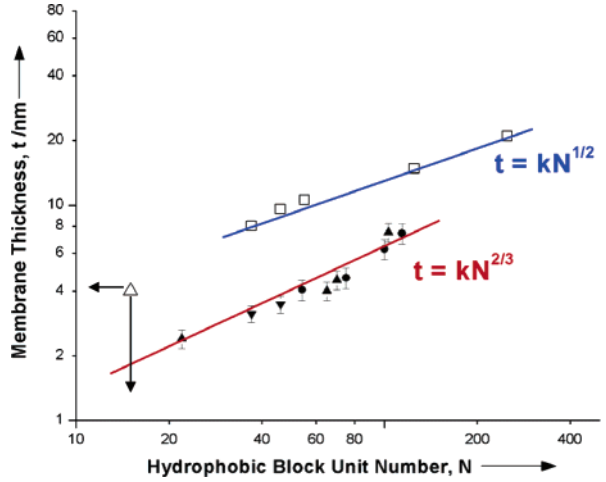

Figure 8. Considering the thickness t and the number of hydrophobic units N and assuming a power law such as $t = kN^b$. Plotting $\ln(t)$ vs $\ln(N)$ both the exponent b and value K can be calculated. (△) Phospholipid membrane, (□) PEO−PB copolymer, ref 24, (▲) E_MB_N diblock copolymers, (▼) $B_NE_MB_N$ triblock copolymer, and (●) $E_MB_NE_M$ triblock copolymers.

copolymers have been shown to self-assemble in bulk according to the strong segregation regime. Accordingly, in the graph in Figure 8, membrane thicknesses are plotted against the number of hydrophobic units. Figure 8 clearly shows that EB vesicles have membrane thickness, t, that scales with the number of hydrophobic units, N, with an exponent, $b \approx 2/3$, i.e., that normally observed in the strong segregation regime. This is in good agreement with their bulk phase behavior. Interestingly, in this highly selective solvent, block copolymers that are not normally ordered in the melt (e.g., $E_{16}B_{22}$) form vesicular lamellar phases that are also found to be in the strong segregation limit.

While the exponent b from the equation

$$t = kN^b \tag{1}$$

used for fitting the data gives an indication of the stretching of the hydrophobic polymer and whether there is strong segregation, the value k depends on the Flory−Huggins parameter χ and therefore on interfacial tension, γ. As already mentioned, the membrane thickness, t, is given by the balance between the interfacial energy of the hydrophobic/hydrophilic boundary and the entropic loss when the polymeric chains are forced into more ordered structures. By minimization of the free energy due to chain stretching, Helfand and Wasserman et al.[38] have estimated a power law for the membrane thickness:

$$t \approx (\gamma a^5/k_bT)^{1/3}N^{2/3} \tag{2}$$

where a is the chain unit length, k_b is Boltzman's constant, and T is temperature. By the same argument, Helfand and Wasserman also assessed the interfacial tension of two incompatible polymers to be dependent on the Flory−Huggins parameter χ;

$$\gamma = \chi^{1/2}k_bT/a^2 \tag{3}$$

Combining eq 2 with eq 3, the equation

$$t \approx a\chi^{1/6}N^{2/3} \tag{4}$$

can be found. Therefore, estimating $k = 0.3$ from the fitting of eq 1 in Figure 8 and substitution in eqs 3 and 4, the Flory−Huggins parameter and the interfacial tension for EB vesicles have been calculated (assuming $a_{PBO} = 0.345$ nm and $T = 298$ K) to be $\chi = 0.43$, and $\gamma = 22.8$ pN/nm, respectively. The Flory−Huggins parameter for the EB block copolymer in bulk state can also be calculated using the equation $\chi_{E-B} = 84.1/T - 0.1120$ from ref 12, which is, at 298 K, $\chi_{E-B} = 0.17$. The solid-state value is obviously smaller than the value calculated for the vesicles; the difference between the two is due to the presence of the preferential solvent, water.

In the same graph, membrane thicknesses reported[28] for vesicles made from polymers with a similar range of molecular weight, the same hydrophile (poly(ethylene oxide)), and the hydrophobic polybutadiene (PEO−PBD) have also been plotted. The PEO−PBD membranes are thicker than EB ones, as expected. The polybutadiene should have a higher interaction parameter χ with both water and the other block PEO, as it is both more hydrophobic than poly(butylene oxide) and more incompatible with PEO. However, the exponent from the fitting of PEO−PBD is surprisingly $b \approx 1/2$, typical of weak segregation or no segregation. This anomaly was explained by the collapse[15] of the PEO chains on the interface between PBD and water, shielding the hydrophobic membrane even further. This extra shielding might be translated as smaller $\chi_{Water-Hydrophobe}$ and therefore smaller interfacial tension. Indeed, the PEO−PBD interfacial tension, $\gamma = 26$ pN/nm, calculated by micromanipulation technique, is very similar to the value calculated here for EB copolymers (22.7 pN/nm) and in contrast to the high difference of hydrophobicity between PBD and PBO.[39] In another work, Srinivas and co-workers[40] have corroborated this weak segregation result by coarse-grain molecular dynamics modeling of the polymeric membranes. The modeling results have confirmed the exponent $b = 0.5$ for membrane thickness higher than 7 nm; however, smaller hydrophobic chains produced an exponent of $b = 0.82$, indicating high chain stretching. This result was explained by calculating the hydrophobic density of the membrane, showing that short chains assemble in a typical β lipid conformation, while at higher molecular weight a more interdigitated arrangement was observed.

The EB membranes studied here appear to be approximately half as thick as the membrane from PEO−PBD of the same molecular weight. In particular, $E_{16}B_{22}$, whose hydrophobic chains are 6 times longer than those of typical phospholipids, makes vesicles with a membrane thickness similar to interdigitated phospholipid membranes (α conformation), which is half the size of typical cell membranes. The work by Schillen[37] et al. on vesicles from amphiphilic polyethers shows that they also have rather thin membranes compared to vesicles with hydrophobes from polybutadiene.

The −C−C−O− backbone of polybutylene oxide is intrinsically more flexible than the −C−C− backbone of phospholipids or polybutadiene. This is borne out by the RIS (rotational isomeric state) calculations of the characteristic ratio C_∞ ($= \langle r^2\rangle_0/$

(38) Helfand, E.; Wasserman, Z. R. In *Developments in Block Copolymers*; Applied Science: London, 1982.
(39) Booth, C.; Yu, G.-E.; Nace, V. M. In *Amphiphilic Block Copolymers: Self-Assembly and Applications*; Paschalis, A., Bjorn, L., Eds.; Elsevier Science Ltd, 2000.
(40) Srinivas, G.; Discher, D. E.; Klein., M. *Nat. Mater.* **2004**, *3*, 6338−6644.

Table 3. Values of Hydrophobic Volumes, Surface Areas per Block, and the Fraction of Bridging for $E_MB_NE_M$ Triblock Copolymers

copolymer	hydrophobe volume,[a] nm^3 $\nu_{PBO} = NM_{wBO}/\rho_{PBO}N_{avogadro}$	surface area per block,[b] nm^2 $A_{molecule} = N\nu_{PBO}/t$	fraction of bridging $\phi_{bridge} = (A_{molecule}/a^2)^{2/3}N^{-1/3}$
$E_{16}B_{22}$	0.027	0.249	n.a.
$E_{50}B_{70}$	0.086	1.333	n.a.
$E_{68}B_{65}$	0.080	1.280	n.a.
$E_{115}B_{103}$	0.127	1.730	n.a.
$B_{37}E_{77}B_{37}$	0.046	0.536	n.a.
$B_{46}E_{99}B_{46}$	0.057	0.763	n.a.
$E_{31}B_{54}E_{31}$	0.067	0.864	0.63
$E_{34}B_{75}E_{34}$	0.092	1.501	0.81
$E_{40}B_{100}E_{40}$	0.123	1.935	0.87
$E_{32}B_{114}E_{32}$	0.141	2.159	0.90

[a] The formula has been taken from ref 45. N is the number of PBO units, M_{wBO} is the molecular weight of the BO monomer, $\rho_{PBO} = 0.97$ g/cm^3 is the density of PBO, and $N_{avogadro}$ is Avogadro's constant. [b]The formula has been taken from ref 45. t is the membrane thickness as calculated in Table 2. The calculation of the surface area per molecule assumes that the diblock passes through the hydrophobe/water interface once and its hydrophobic end is buried. This is also the case for the $B_NE_MB_N$, which was treated as the equivalent diblock with $B_NE_{M/2}$, whereas the $E_MB_NE_M$ passes through the interface twice with either an I or a U conformation.

nl^2, the ratio of the measured unperturbed dimensions to the equivalent freely jointed chain) for polyethylene oxide and polyethylene, being 4 and 6.7, respectively.[41] That PBO blocks are more easily coiled that PBD blocks can be used to explain the absolute difference in membrane thickness seen in Figure 8. The relative thickness of the hydrophobic membranes should scale with their radii of gyration and to zeroth-order approximation their characteristic ratio. Obviously the relative lack of flexibility in a phospholipid chain would cause the bilayer morphology to be preferred—the configurational entropy does not necessarily drive layer mixing in this case—but it is difficult to imagine a stretched conformation of a pair of hydrophobic polymer brushes that would not be mixed or interdigitated, and this is borne out by the vast experimental and theoretical literature on block copolymer lamellae. As evidence, the membrane thicknesses of both $B_NE_MB_N$ and $E_MB_NE_M$ triblock copolymers fit the same trend as the E_MB_N diblock copolymers. Hydrophobic−hydrophilic−hydrophobic $B_NE_MB_N$ copolymers are similar to diblock copolymers in that there is only one molecular conformation consistent with membrane formation; they have hydrophobic chain ends assembled into a membrane and the hydrophilic block must form a loop. In this case both hydrophilic−hydrophobic junctions are on the same side of the membrane. Conversely hydrophilic−hydrophobic−hydrophilic $E_MB_NE_M$ copolymers can have two possible conformations in the membrane, depending on whether the hydrophobic chain makes a loop and the hydrophilic chains are on the same side of the membrane (U-shape) or whether the molecule bridges the hydrophobic membrane with hydrophilic chains on opposite sides (I-shape).[42]

The fraction of bridging chains, at equilibrium, has been evaluated by theoretical calculation based on self-consistent-field (SCF) theories[43] and later confirmed experimentally by dielectric relaxation measurements.[44] The reported formula allows calculation of the fraction of bridging chains in triblock assemblies, $\phi_{bridge} \approx (A_{molecule}/a^2)^{2/3}N^{-1/3}$, where $A_{molecule}$ is the surface area per block, a is the chain unit length, and N is the PBO unit number. In Table 3 the hydrophobe volumes, the surface areas per block, calculated here using the method reported by Förster et al.,[45] and the fraction of bridging for $E_MB_NE_M$ triblocks are listed. Calculations show clearly that triblocks and diblocks have similar surface areas per molecule, confirming high similarities between $E_MB_NE_M$ triblock packing and diblocks and $B_NE_MB_N$ triblocks.

The calculations of the fraction of bridging show clearly that the majority of the $E_MB_NE_M$ triblocks prefer to bridge. This strongly indicates that $E_MB_NE_M$ membranes are completely interdigitated. The consequent conclusion, arising from $E_MB_NE_M$ triblock membrane thicknesses falling onto the same master curve as diblocks and $B_NE_MB_N$ triblocks, is that EB vesicles all have an interdigitated membrane analogous to that of interdigitated phospholipid membranes (α conformation). The theoretical and modeling work by Srinivas[40] also suggests that there is an increasing tendency for layer mixing and interdigitation at higher molecular weights. The coarse grained models show that the "methyl trough", a characteristic of true bilayer formation, is not observed when the degree of polymerization in the hydrophobe is more than 18, and all but the smallest molecules studied here have a higher value than this. Therefore we would expect the polymer brushes to be mixed. The calculated area per molecule in Table 3 compares well with the model with no "methyl trough". For example, Srinivas predicts the area per molecule to be 1.46 nm^2 for $EO_{73}EE_{71}$, and we measure 1.28 nm^2 for a comparable molecule $E_{68}B_{65}$.

Experimental Section

Materials. Copolymers were prepared by sequential anionic copolymerization and were characterized using gel permeation chromatography and ^{13}C NMR spectroscopy as described elsewhere.[12] Molecular details of the copolymers are presented in Table 1, where f_E is the volume fraction of the poly(ethylene oxide) block and M_w is the block copolymer molecular weight calculated by GPC and ^{13}C NMR. Rhodamine B octadecyl ester perchlorate amphiphilic fluorescent dye, chloroform, and uranyl acetate were supplied by Aldrich-Sigma Ltd.

Vesicle Preparation. Block copolymers are first dissolved in chloroform at a concentration of 4 mg/mL. For microscale vesicles, block copolymers were deposited onto two platinum electrodes (20 × 5 × 2 mm) by evaporation from chloroform solution. The electrodes were immersed in distilled water, and an ac electric field, 10 V and 10 Hz, was applied. Details of the experimental setup are given elsewhere.[32] For nanoscale vesicles, the solution is placed into glass vials; the

(41) Flory, P. J. *The Statistical Mechanics of Chain Molecules*; Interscience Publishers−John Wiley: New York, 1969.
(42) Napoli, A.; Tirelli, N.; Wehrli, E.; Hubbell, J. A. *Langmuir* **2002**, *18*, 8324−8329.
(43) Zhulina, E. B.; Halperin, A. *Macromolecules* **1992**, *25*, 5730−5741.
(44) Watanabe, H. *Macromolecules* **1995**, *28*, 5006−5011.
(45) Förster, S.; Berton, B.; Hentze, H.-P.; Krämer, E.; Antonietti, M.; Linder, P. *Macromolecules* **2001**, *34*, 4610−4623.

chloroform is then evaporated by vacuum, leading to the formation of a copolymeric film onto the vial walls. Deionized water is subsequently added to the vial, and the vial is stirred for at least 1 day. To narrow the particle size distribution, vesicle dispersions obtained were extruded through a LiposoFast-Basic polycarbonate membrane. The sample is passed 10 times through the membrane by pushing the sample back and forth between two syringes. Alternately, the vesicle dispersion is sonicated for a few hours using a sonicator from the Sonicor Instrument Corporation. All the solvents are filtered and the glassware is washed with filtered solvent before the vesicle preparation.

Characterization. Dynamic light scattering measurements were performed on a Brookhaven Instruments 200SM laser light scattering goniometer using a He−Ne 125 mW 633 nm laser. The vesicle dispersions are placed into glass vials. Single scans of 10 min exposure were performed on the sample. Particle sizes were estimated using the non-negative least square (NNLS) multiple pass method of data analysis. Confocal laser scanning microscopy was performed using a ZEISS LSM 510M; vesicle membranes were generated in the presence of a small amount (0.1−0.2% w/$w_{copolymer}$) of Rhodamine B octadecyl ester perchlorate. Transmission electron microscopy was performed using Philips CM100 and CM200 equipped with a Gatan 1k CCD camera. For freeze-dried specimens, an aluminum bar is immersed into liquid nitrogen for at least half an hour. The grids are engrossed into the sample and then placed onto the cold metallic bar. The bar with the grids is quickly positioned into a vacuum oven, where the grids are kept under vacuum at room temperature overnight. For negative-stained specimens, the grids are submerged for 20 s into the sample solution and then in a uranyl acetate water solution (2% w/w). The grids are subsequently dried under vacuum. Cryogenic TEM specimens were prepared by fast immerging a pre-sample-engrossed grid in liquid ethane. The grid is quickly placed in a cryogenic stage and kept at −170 °C. SAXS experiments were performed on a beam line 6.2 of the Synchrotron Radiation Source (SRS) at the Daresbury Laboratory, Warrington U.K. The beam line is configured for SAXS experiments using monochromatic radiation of 1.4 Å wavelength.[46] Data are analyzed using inverted Fourier transform on the GIFT software package.

Conclusion

In the present contribution, it has been shown that EB copolymers are able to self-assemble into very stable vesicles but also that vesicles are the main aggregate formed under the applied conditions. Very few nonvesicular aggregates have been observed by DLS, TEM, and SAXS.

The resolution of the differences between the present data and those published previously for polybutadiene membranes is the inherent flexibility of polyethers. Specifically the difference in the characteristic ratios of polyether versus alkyl chains explains the absolute difference in membrane thickness, because PBO blocks are more easily coiled that PBD blocks. Moreover we find that the relationship between the hydrophobic membrane thickness and molecular weight is that expected for the strong segregation limit. An exponent of 2/3 is observed for polyether hydrophobes, but this is in contrast to the value of 1/2 previously reported[28] for polybutadiene. The difference in the absolute value of the membrane thickness for the different polymers in Figure 8 can be ascribed to their chemical differences; that is, the higher flexibility of the polyether accounts for its thinner membranes, and this is borne out by systematic differences in the area per molecule. What is still not clear is the reasons for the 1/2 dependence in the polybutadiene membranes[28] when the same group have observed the more consistent molecular weight scaling of 0.61 for the diameter of the hydrophobe in wormlike micelles.[27]

Finally, we question the usefulness of the nomenclature of bilayers and interdigitation when applied to block copolymer vesicles. The behavior of block copolymer lamellae in the melt clearly shows that the two stretched brushes, emanating from the interfaces and comprising each domain, are mixed for entropic reasons.[16] Obviously the relative lack of flexibility in a phospholipid chain can cause the bilayer morphology to be preferred. The configurational entropy does not necessarily drive layer mixing in this case, but there are no compelling reasons why two hydrophobic polymer brushes[12−14] would separate. This is borne out by the measurements presented here. The EB copolymers have been shown to form membranes whose architecture is the result of the coiling and interdigitation of the hydrophobic polybutylene oxide and agrees with previously published SCFT calculations[16] that show that the majority of chain-ends are buried beyond the mid-plane for finite values of χN. The picture presented here is not, however, an interdigitated membrane that leads to water exposure of every hydrophobic block at both the block junction and the other end of the PBO chain. While this might be the case for interdigitated lipids, we suggest that block copolymer brushes are entangled with buried chain-ends rather than being either a definite interdigitated monolayer or a well-separated bilayer. We suggest that the phospholipid description of the well-separated hydrophobic bilayer and the completely interdigitated monolayers are extreme boundary conditions and are not always appropriate to describe the more subtle structure of block copolymer vesicles or polymersomes.

Acknowledgment. The authors would like to thank the ICI Strategic Technology Group for financial support. We acknowledge the contributions of Dr. Shao-Min Mai, who synthesized the block copolymers used in the present work, Dr. Oleksandr Mykhaylyk for stimulating discussions of scattering data analysis, and Dr. Mark Matsen for pointing us to the relevant theoretical work.

JA050742Y

(46) Cernik, R. J.; Barnes, P.; Greaves, G. N.; Rayment, T.; Ryan, A. J. *Appl. Crystallogr.* **2004**, *19th*, 3−9.